

Target-Induced and Equipment-Free DNA Amplification with a Simple Paper Device

Meng Liu, Christy Y. Hui, Qiang Zhang, Jimmy Gu, Balamurali Kannan, Sana Jahanshahi-Anbuhi, Carlos D. M. Filipe, John D. Brennan,* and Yingfu Li*

Abstract: We report on a paper device capable of carrying out target-induced rolling circle amplification (RCA) to produce massive DNA amplicons that can be easily visualized. Interestingly, we observed that RCA was more proficient on paper than in solution, which we attribute to a significantly higher localized concentration of immobilized DNA. Furthermore, we have successfully engineered a fully functional paper device for sensitive DNA or microRNA detection via printing of all RCA-enabling molecules within a polymeric sugar film formed from pullulan, which was integrated with the paper device. This encapsulation not only stabilizes the entrapped reagents at room temperature but also enables colorimetric bioassays with minimal steps.

There is currently a great need for developing rapid and effective point-of-care (POC) diagnostics that can improve patient care in resource-limited settings.^[1] Paper-based POC diagnostic devices provide a platform for portable, low-cost, low-volume, disposable, and simple sensors,^[2] which can be developed using inkjet printing,^[3] wax printing^[4] or screen printing technology,^[5] making them amenable to automated fabrication or even on-site production in areas with limited resources.^[6]

One major challenge in paper-based diagnostics is to integrate molecular amplification technology to allow sensitive target detection. Recently, isothermal nucleic acid amplification techniques have been widely investigated as a method to facilitate target or signal amplification in molecular biology and bioanalysis without the use of thermocycling devices.^[7] Thus the combination of isothermal nucleic acid amplification techniques with paper-based POC diagnostics should add critical functionality to these devices to make them more robust and sensitive.^[8]

Herein, we describe rolling circle amplification (RCA), a simple and efficient isothermal enzymatic DNA replication process,^[9] that is performed in a microzone plate fabricated on a paper substrate (paper-based RCA) using wax printing, and provide a theoretical basis for understanding the nucleic acid amplification reaction on paper, and in particular, the intriguing finding that RCA efficiency on paper is enhanced relative to solution. We further demonstrate an “all-in-one” paper-based amplification system, in which all required reagents for amplification and detection are integrated via printing into the sensor, providing improved functionality and ease of use.

To make a paper device for RCA, we chose to print a preformed 5'-biotinylated DNA-streptavidin conjugate onto a nitrocellulose membrane surface (see Supporting Information (SI) for details), which is known to have high affinity for protein binding. Importantly, the sequence of the printed DNA molecule was designed to be complementary to part of a circular DNA template (CDT) and thus can act as a primer for RCA. To demonstrate that the proposed strategy allows efficient printing of DNA primers onto a paper surface, we performed the following experiment. We first used the wax-printing technique to produce a 96-microzone paper plate, with the diameter of each test zone being 4 mm. A fluorescently labeled DNA-streptavidin conjugate was then printed onto each test zone using a piezoelectric microarray printer. Using measured fluorescence intensity (Figure 1), we calculated a molecular density of ca. $2.5 \times 10^{13} \text{ cm}^{-2}$ on each test zone, which is reasonably consistent with the theoretically predicted value of $8 \times 10^{12} \text{ cm}^{-2}$ ($\rho = 1/\pi r^2$; $r = 4 \text{ nm}$, representing the diameter of streptavidin).

We then produced a similar 96-microzone paper device using non-fluorescently labeled primer TP1. We performed RCA on paper by placing on a microzone a mixture of circular DNA template (CDT1 or CDT2; see below), phi29 DNA polymerase ($\phi 29\text{DP}$), dNTPs and reaction buffer, followed by incubation at room temperature for 40 min (see SI for details). Four different methods were used to confirm the formation of RCA products (RP) on paper. First,

[*] Dr. M. Liu, J. Gu, Prof. Dr. Y. Li

Departments of Biochemistry and Biomedical Sciences and Chemistry & Chemical Biology, McMaster University
1280 Main Street West, Hamilton, ON, L8S 4K1 (Canada)
E-mail: liying@mcmaster.ca

C. Y. Hui, Dr. Q. Zhang, Dr. B. Kannan, Prof. Dr. C. D. M. Filipe, Prof. Dr. J. D. Brennan, Prof. Dr. Y. Li
Biointerfaces Institute, McMaster University
1280 Main Street West, Hamilton, ON, L8S 4L8 (Canada)
E-mail: brennanj@mcmaster.ca

Dr. S. Jahanshahi-Anbuhi, Prof. Dr. C. D. M. Filipe
Department of Chemical Engineering, McMaster University
1280 Main Street West, Hamilton, ON, L8S 4L7 (Canada)

Supporting information for this article is available on the WWW under <http://dx.doi.org/10.1002/ange.201509389>.

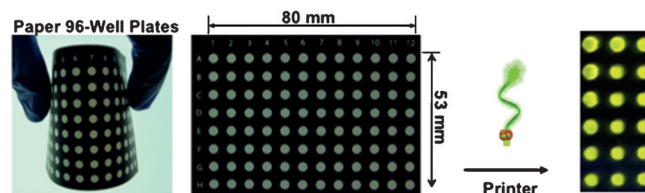


Figure 1. Image of a paper plate made of 96 microzones printed with fluorescent DNA-streptavidin conjugates.

[α - 32 P]dGTP was added in the reaction mixture so that the RP became radioactive (Figure 2A). Second, a fluorophore-labeled DNA probe (DP1) that can hybridize with the RP was used to produce a fluorescence signal (Figure 2B). Third, gold nanoparticles (AuNPs) functionalized with a complementary DNA probe (DP2) was used to produce a colorimetric signal (Figure 2C). Note that in these three assays we used the same circular DNA template CDT1. However, in the final assay, we used a modified CDT1, named CDT2, which was designed to produce a special RP containing repetitive units of a peroxidase-mimicking DNAzyme, PW17, that was able to generate a colorimetric signal (Figure 2D).^[10] Following RCA, the reaction mixture was also taken and placed in a test-tube. No color change was observed (Figure S1 in the SI), suggesting that the RP is indeed paper-bound. Taken together, these tests demonstrated that the RCA reaction could be performed on paper printed with a DNA primer.

We next investigated RCA performance on paper relative to solution. In order to quantify the long RP on paper, we designed a new DNA primer (TP2) that contained two sequence domains: a 5' domain that binds to a DNA capture sequence (DC1) printed onto paper microzones and a 3' domain complementary to the circular template CDT2. After the RCA reaction, we added urea to elute the RP from the paper surface. The recovered RP, which contained a recognition sequence for the restriction enzyme *EcoRV*, was converted into monomers using *EcoRV*. Fully digested RP was then analyzed by denaturing polyacrylamide gel electrophoresis (PAGE). A full monomerization (60 nt) of RP was achieved after a 24-hour digestion (Figure S2 in the SI).

Through the use of a 50-nt DNA molecule with a defined concentration as an internal control, we were able to determine the fluorescence ratio (FR) of the two bands in each lane (Figure 3A), and calculate the average repeating units (ARUs) in the RP (see SI for details).

We applied this method to compare the efficiency of solution-based RCA using free TP2 (F-TP2) and solid-phase RCA using paper-bound TP2 (P-TP2). Figure 3B shows the time-dependent ARU values for the two RCA strategies. It was observed that the overall ARUs of paper-based RCA were much higher than that of solution-based RCA. This result highlights the enticing advantage of paper-based RCA in terms of reaction kinetics, implying that the rate of the enzymatic reaction was faster on paper.

The efficiency of RCA is highly dependent on the number and thermal stability (T_m) of primer–template duplexes. In general, the T_m of a DNA duplex is positively correlated with the localized concentrations of hybridizing DNA strands.^[11] For a solution-based RCA system that consists of 10 nM TP and CDT, the volume of a sphere containing one DNA molecule would be 0.17 fL (Figure 3C, see SI for details), and thus the calculated sphere radius is about 340 nm. For the paper-based RCA strategy, the immobilization process will confine each DNA partner within a hemisphere of less than 10 nm in radius considering its length. Thus the volume of the hemisphere would be 2.1 zL. Under these conditions, the localized concentration of these DNA molecules is estimated to be 800 μ M, or 80000-fold higher than in solution. This should increase the estimated T_m for the TP-CDT duplex from 48 °C to 67 °C with the increase of effective concen-

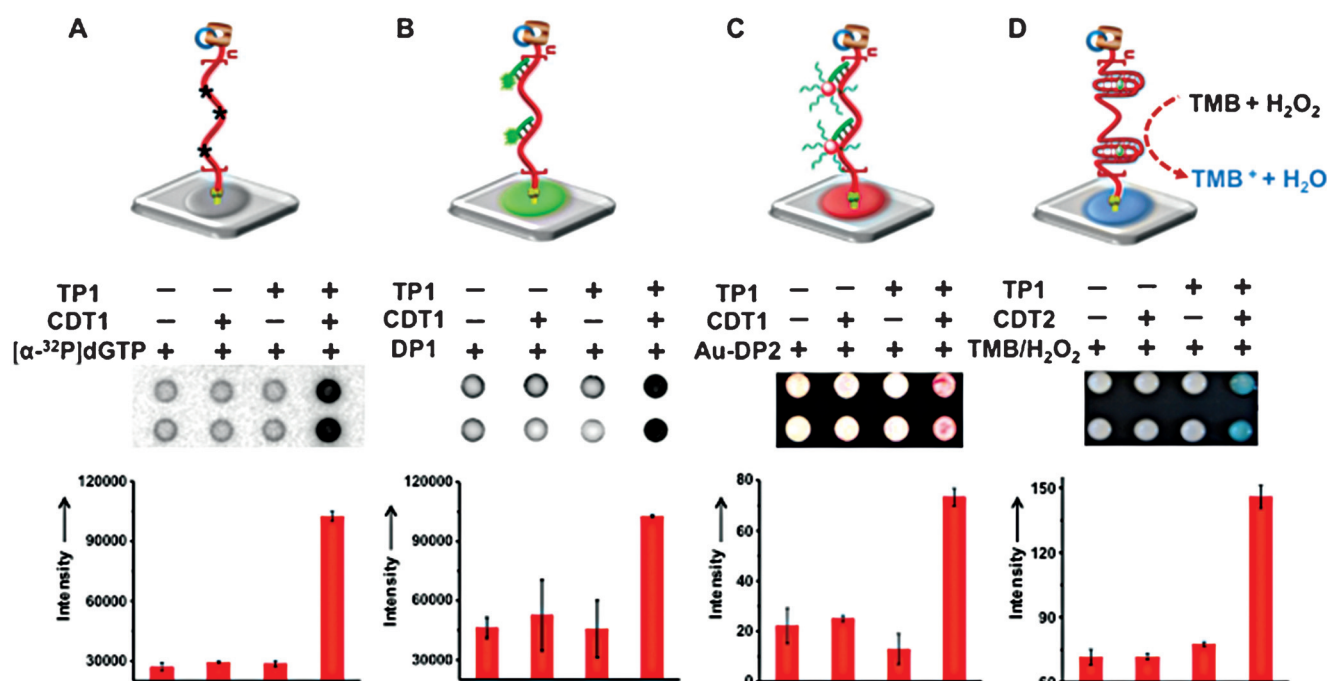


Figure 2. Performing RCA with paper-bound primer. Detection of RCA products (RP) through: A) incorporation of radioactive tracer into DNA chain; B) fluorescent assay using a fluorophore-labeled DNA oligonucleotide (note that the higher background is attributed to the nonspecific binding and the fluorescence background of paper); C) colorimetric assay using AuNP–DNA conjugates; D) colorimetric assay by a peroxidase-mimicking DNAzyme through the oxidation of 3,3',5,5'-tetramethylbenzidine (TMB) in the presence of hemin and H₂O₂.

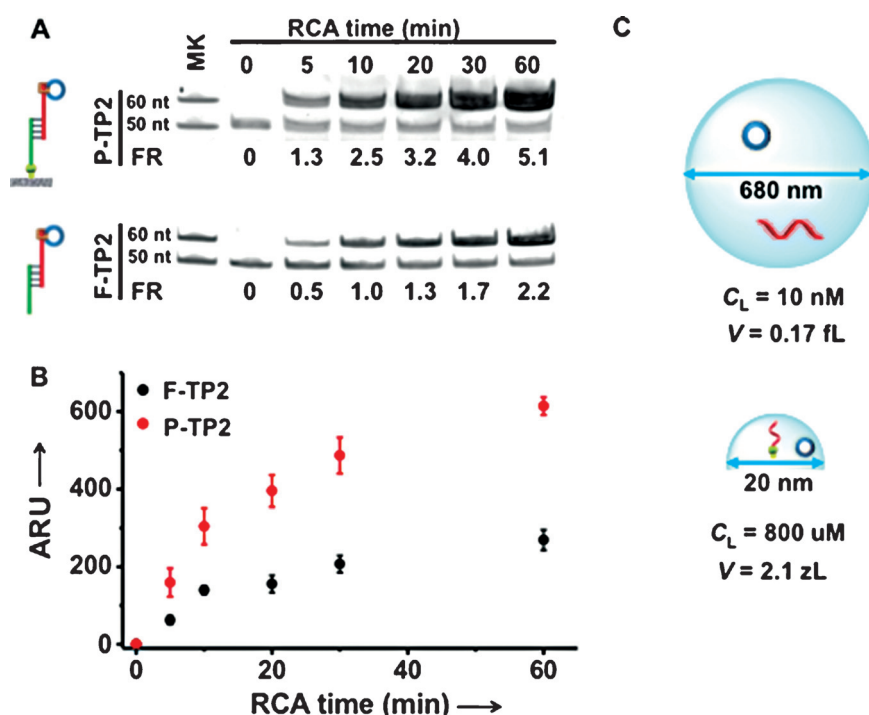


Figure 3. Determination of RCA efficiency. A) dPAGE analysis of digested RP obtained at varying RCA times with free TP2 (F-TP2) and paper-bound TP2 (P-TP2). Top band: digested RCA monomer (60 nt). Bottom band: DNA loading control (50 nt). FR: ratio of fluorescence intensity of the 60-nt and 50-nt DNA bands. ARU: average repeating units of RP from a given circular template. B) Average repeating units (ARU) of RP vs. RCA time for F-TP2 and P-TP2. C) Schematic illustration showing that the immobilization of DNA primers on paper substantially increases the localized concentrations of the primer–circular template complex.^[11]

tration from 10 nM to 800 μM under the conditions of 100 mM NaCl and 5 mM MgCl_2 at 30 °C, making the RCA process more effective on paper.

Two additional experiments were conducted to further confirm the increased efficiency of paper-based RCA. The first experiment examined the effect of TP2 concentration on RCA efficiency and the results (Figure S3A in the SI) demonstrate that increasing primer concentration has more profound effect on solution-based RCA than paper-based RCA. The second experiment involved the use of a longer primer, TP3, designed to increase the T_m of primer–template duplex (65 °C for TP3 and 48 °C for TP2). It was found that TP3 significantly boosted the efficiency of solution-based RCA but had a much smaller effect on paper-based RCA (Figure S3B in the SI). These observations confirm the role of immobilization in improving the thermal stability of primer–template duplex, thus facilitating the RCA reaction on paper.

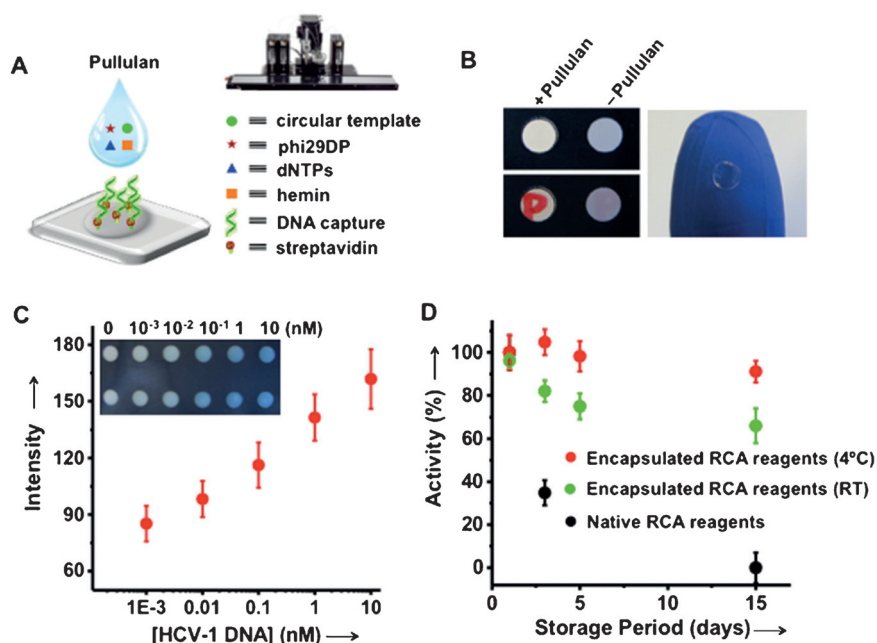


Figure 4. A) Schematic diagram of the preparation of all-in-one paper-based amplification system using pullulan. B) Typical images of pullulan tablets. C) Dose–response curves for HCV-1 DNA detection with the bioactive paper sensor. Inset: a photograph for visual detection on a chip array at HCV-1 at various concentrations. Two rows represent two repeats. D) Evaluation of the long-term stability of the paper sensors stored at 4 °C and room temperature (RT).

dNTPs and hemin, 3) printing the above mixture into the circular test zones as described previously,^[17] and 4) air-drying (see SI for details). The transparent pullulan films (letter “P” can be seen) with the encapsulated RCA reagents are obtained on the paper array after drying (Figure 4B). Addition of a DNA or RNA target leads to the formation of a DC2/CDT3/target complex, which enables the RCA reaction. The RP produced can be detected colorimetrically. We note that the current device requires several sample preparation steps prior to addition of the test sample to the paper device. More efficient on-paper sample preparation strategies, such as the DNA extraction method described by Govindarajan et al., are required to further simplify the assay.^[18]

We utilized this method for the detection of single-stranded HCV-1 DNA (a portion of DNA sequence from the hepatitis C virus genome) to demonstrate analyte-triggered RCA and subsequent detection on paper. As shown in Figure 4C, RP was observed upon addition of the target, producing colorimetric signals that were proportional to the target concentration, with data calculated using ImageJ. In the absence of HCV-1 DNA, the RCA reaction was not initiated (Figure S4 in the SI). The sensor provided a detection limit of 10 pM on the basis of the 3σ /slope (σ , standard deviation of the blank samples), demonstrating the key advantage of amplification on paper, and showed excellent selectivity against unintended targets HCV-M1 and HCV-M2 with mutations in the HCV-1 sequence (Figure S5 in the SI). The positive results further indicate that pullulan does not interfere with the RCA reaction (Figure S6 in the SI).

We also evaluated the long-term stability of the “all-in-one” amplification system. As shown in Figure 4D, RCA reagents stored in solution at room temperature lost $65 \pm 6\%$ activity within three days and become completely inactive within 15 days. In contrast, RCA reagents within pullulan films retained $91 \pm 5\%$ and $66 \pm 8\%$ of their initial activity after storage at 4°C and room temperature for 15 days, respectively. This result clearly shows that the biomolecules can be effectively protected from thermal denaturation or chemical modification after pullulan encapsulation. This feature is encouraging for room-temperature shipping and storage of the paper-based sensors.

To demonstrate the analytical utility of the paper based RCA system, the sensor was used to detect microRNAs (miRNAs), a group of short (19–25 nucleotides) and endogenous non-protein-coding RNAs, which are promising biomarkers in clinical diagnosis and therapy.^[19] We employed the “all-in-one” amplification system to measure the absolute amounts of hsa-miR-21 (miR-21) in enriched small RNA (<200 nt) extracted from human breast cancer cell line (MCF-7) and normal mammary epithelial cell line (MCF-10A). Studies have indicated that miR-21 is one of the most abundant miRNAs over-expressed in numerous tumor tissues.^[20] The contents of miR-21 in these two cell lines were estimated by the standard addition method and the value of miR-21 was compared with the result of the qRT-PCR method (Figure S7 and S8 in the SI). It was determined that the absolute amount of miR-21 found in MCF-7 and MCF-10A cells were 30.7×10^5 copies/ng RNA (or 5400 copies/cell)

and 6.6×10^5 copies/ng RNA (or 250 copies/cell), respectively, which are comparable with the values obtained using qRT-PCR (Table 1), thus demonstrating the reliability of our assay.

Table 1: miR-21 amounts (copies/ng RNA $\times 10^5$) in extracted total small RNA from MCF-7 and MCF-10A cell lines.

Cell line ^[a]	Paper-based assay	qRT-PCR ^[b]	Total small RNA (< 200 nt, μ g)
MCF-7	30.7 ± 5.2	12.5 ± 3.5	17.6
MCF-10A	6.6 ± 1.3	2.3 ± 1.1	3.7

[a] The number of cultured cell is about 1×10^7 . [b] 15 ng of total small RNA per assay. Data are averages \pm SD of three independent experiments.

Overall, our work demonstrates that the RCA reaction can be performed on a patterned paper device, with the reaction operating with enhanced kinetics, producing rapid and sensitive POC diagnostics. This work also demonstrates that enhanced local reagent concentrations can actually improve RCA performance relative to solution. Our work further demonstrates that pullulan materials provide both a suitable reagent depot to allow stabilization of labile (bio)reagents and a simple method to immobilize such reagents on paper. The paper sensor with integrated amplification is shown to be suitable for carrying out colorimetric bioassays with minimal steps and without the need for special reagent handling, making this approach particularly suitable for POC testing in resource-limited settings.

Acknowledgements

Funding was provided by the Natural Sciences and Engineering Council of Canada, Pro-Lab Diagnostics, the Canada Foundation for Innovation, and the Ontario Ministry of Research and Innovation through an Ontario Research Fund grant. Part of the work was conducted at the McMaster Biointerfaces Institute.

Keywords: biosensor · paper · point of care diagnostics · pullulan · rolling circle amplification

How to cite: *Angew. Chem. Int. Ed.* **2016**, *55*, 2709–2713
Angew. Chem. **2016**, *128*, 2759–2763

- [1] a) P. Yager, G. J. Domingo, J. Gerdes, *Annu. Rev. Biomed. Eng.* **2008**, *10*, 107–144; b) D. A. Giljohann, C. A. Mirkin, *Nature* **2009**, *462*, 461–464; c) M. Urdea, L. A. Penny, S. S. Olmsted, M. Y. Giovanni, P. Kaspar, A. Shepherd, P. Wilson, C. A. Dahl, S. Buchsbaum, G. Moeller, D. C. Hay Burgess, *Nature* **2006**, *444*, 73–79; d) P. Yager, T. Edwards, E. Fu, K. Helton, K. Nelson, M. R. Tam, B. H. Weigl, *Nature* **2006**, *442*, 412–418; e) L. Kulinsky, Z. Noroozi, M. Madou, *Methods Mol. Biol.* **2013**, *949*, 3–23.
- [2] a) A. W. Martinez, S. T. Phillips, G. M. Whitesides, *Anal. Chem.* **2010**, *82*, 3–10; b) X. Li, D. R. Ballerini, W. Shen, *Biomicrofluidics* **2012**, *6*, 011301; c) A. K. Yetisen, M. S. Akram, C. R. Lowe, *Lab Chip* **2013**, *13*, 2210–2251; d) C. Parolo, A. Merkoçi, *Chem. Soc. Rev.* **2013**, *42*, 450–457; e) D. D. Liana, B. Raguse, J. J. Gooding, E. Chow, *Sensors* **2012**, *12*, 11505–11526.

- [3] S. Su, M. M. Ali, C. D. Filipe, Y. Li, R. Pelton, *Biomacromolecules* **2008**, *9*, 935–941.
- [4] E. Carrilho, A. W. Martinez, G. M. Whitesides, *Anal. Chem.* **2009**, *81*, 7091–7095.
- [5] A. Savolainen, Y. Zhang, D. Rochefort, U. Holopainen, T. Erho, J. Virtanen, M. Smolander, *Biomacromolecules* **2011**, *12*, 2008–2015.
- [6] a) C. M. Cheng, A. W. Martinez, J. Gong, C. R. Mace, S. T. Phillips, E. Carrilho, K. A. Mirica, G. M. Whitesides, *Angew. Chem. Int. Ed.* **2010**, *49*, 4771–4774; *Angew. Chem.* **2010**, *122*, 4881–4884; b) A. W. Martinez, S. T. Phillips, G. M. Whitesides, *Proc. Natl. Acad. Sci. USA* **2008**, *105*, 19606–19611; c) H. Liu, Y. Xiang, Y. Lu, R. M. Crooks, *Angew. Chem. Int. Ed.* **2012**, *51*, 6925–6928; *Angew. Chem.* **2012**, *124*, 7031–7034; d) S. M. Z. Hossain, C. Ozimok, C. Sicard, S. D. Aguirre, M. M. Ali, Y. Li, J. D. Brennan, *Anal. Bioanal. Chem.* **2012**, *403*, 1567–1576; e) A. W. Martinez, S. T. Phillips, M. J. Butte, G. M. Whitesides, *Angew. Chem. Int. Ed.* **2007**, *46*, 1318–1320; *Angew. Chem.* **2007**, *119*, 1340–1342.
- [7] a) J. Li, J. Macdonald, *Biosens. Bioelectron.* **2015**, *64*, 196–211; b) K. P. F. Janssen, K. Knez, D. Spasic, J. Lammertyn, *Sensors* **2013**, *13*, 1353–1384; c) L. Yan, J. Zhou, Y. Zheng, A. S. Gamson, B. T. Roembke, S. Nakayama, H. O. Sintim, *Mol. Biosyst.* **2014**, *10*, 970–1003.
- [8] a) C. Jung, A. D. Ellington, *Acc. Chem. Res.* **2014**, *47*, 1825–1835; b) L. M. Zanolli, G. Spoto, *Biosensors* **2013**, *3*, 18–43; c) A. Niemz, T. M. Ferguson, D. S. Boyle, *Trends Biotechnol.* **2011**, *29*, 240–250; d) P. Craw, W. Balachandran, *Lab Chip* **2012**, *12*, 2469–2486; e) P. J. Asiello, A. J. Baumnner, *Lab Chip* **2011**, *11*, 1420–1430.
- [9] a) A. Fire, S. Q. Xu, *Proc. Natl. Acad. Sci. USA* **1995**, *92*, 4641–4645; b) D. Liu, S. L. Daubendiek, M. A. Zillman, K. Ryan, E. T. Kool, *J. Am. Chem. Soc.* **1996**, *118*, 1587–1594; c) W. Zhao, M. M. Ali, M. A. Brook, Y. Li, *Angew. Chem. Int. Ed.* **2008**, *47*, 6330–6337; *Angew. Chem.* **2008**, *120*, 6428–6436; d) M. M. Ali, F. Li, Z. Zhang, K. Zhang, D. K. Kang, J. A. Ankrum, X. C. Le, W. Zhao, *Chem. Soc. Rev.* **2014**, *43*, 3324–3341.
- [10] a) P. Travascio, Y. Li, D. Sen, *Chem. Biol.* **1998**, *5*, 505–517; b) H. Z. He, D. S. Chan, C. H. Leung, D. L. Ma, *Nucleic Acids Res.* **2013**, *41*, 4345–4359; c) Z. Cheglakov, Y. Weizmann, B. Basnar, I. Willner, *Org. Biomol. Chem.* **2007**, *5*, 223–225.
- [11] Q. Zhang, F. Li, B. Dever, C. Wang, X. F. Li, X. C. Le, *Angew. Chem. Int. Ed.* **2013**, *52*, 10698–10705; *Angew. Chem.* **2013**, *125*, 10894–10902.
- [12] a) J. Ninio, *Proc. Natl. Acad. Sci. USA* **1987**, *84*, 663–667; b) M. Salas, *Annu. Rev. Biochem.* **1991**, *60*, 39–71.
- [13] a) L. Blanco, A. Bernad, J. M. Lharo, G. Martin, C. Garmendia, M. Salas, *J. Biol. Chem.* **1989**, *264*, 8935–8940; b) L. Blanco, J. M. Lazaro, M. D. Vega, A. Bonnin, M. Salas, *Proc. Natl. Acad. Sci. USA* **1994**, *91*, 12198–12202.
- [14] a) P. B. Gaspers, C. R. Robertson, A. P. Gast, *Langmuir* **1994**, *10*, 2699–2704; b) P. B. Gaspers, A. P. Gast, C. R. Robertson, *J. Colloid Interface Sci.* **1995**, *172*, 518–529; c) G. Trigiante, A. P. Gast, C. R. Robertson, *J. Colloid Interface Sci.* **1999**, *213*, 81–86.
- [15] R. C. Rodrigues, C. Ortiz, A. Berenguer-Murcia, R. Torres, R. Fernandez-Lafuente, *Chem. Soc. Rev.* **2013**, *42*, 6290–6307.
- [16] S. Jahanshahi-Anbuhi, K. Pennings, V. Leung, M. Liu, C. Carrasquilla, B. Kannan, Y. Li, R. Pelton, J. D. Brennan, C. D. Filipe, *Angew. Chem. Int. Ed.* **2014**, *53*, 6155–6158; *Angew. Chem.* **2014**, *126*, 6269–6272.
- [17] B. Kannan, S. Jahanshahi-Anbuhi, R. H. Pelton, Y. Li, C. D. M. Filipe, J. D. Brennan, *Anal. Chem.* **2015**, *87*, 9288–9293.
- [18] A. V. Govindarajan, S. Ramachandran, G. D. Vigil, P. Yager, K. F. Böhringer, *Lab Chip* **2012**, *12*, 174–181.
- [19] a) L. He, G. J. Hannon, *Nat. Rev. Genet.* **2004**, *5*, 522–531; b) S. L. Ameres, P. D. Zamore, *Nat. Rev. Mol. Cell Biol.* **2013**, *14*, 475–488; c) B. M. Ryan, A. I. Robles, C. C. Harris, *Nat. Rev. Cancer* **2010**, *10*, 389–402; d) H. Dong, J. Lei, L. Ding, Y. Wen, H. Ju, X. Zhang, *Chem. Rev.* **2013**, *113*, 6207–6233; e) J. Li, S. Tan, R. Kooger, C. Zhang, Y. Zhang, *Chem. Soc. Rev.* **2014**, *43*, 506–517.
- [20] A. M. Krichevsky, G. Gabriely, *J. Cell. Mol. Med.* **2009**, *13*, 39–53.

Received: October 10, 2015

Revised: December 2, 2015

Published online: January 8, 2016